Hall effect in incompressible magnetic reconnection

Laura F. Morales, Sergio Dasso, and Daniel O. Gómez

Instituto de Astronomía y Física del Espacio (IAFE), Departamento de Física, Facultad de Ciencias Exactas y Naturales, Universidad de Buenos Aires, Buenos Aires, Argentina

Received 9 July 2004; revised 3 January 2005; accepted 13 January 2005; published 9 April 2005.

[1] Theoretical models of magnetic reconnection have been traditionally developed within the framework of magnetohydrodynamics (MHD). However, in low-density astrophysical plasmas like those found in the magnetopause and the magnetotail, kinetic effects such as the Hall current are expected to play a significant role. We present results from externally driven magnetic reconnection simulations, within the framework of incompressible Hall MHD in 2 1/2 dimensions. We evaluate the relevance of the Hall current in the reconnection process by performing a set of simulations with different values of the Hall parameter. We compute the corresponding reconnection rates as a function of time and explore the spatial structure of the fields in the surroundings of the diffusion region.

Citation: Morales, L. F., S. Dasso, and D. O. Gómez (2005), Hall effect in incompressible magnetic reconnection, *J. Geophys. Res.*, *110*, A04204, doi:10.1029/2004JA010675.

1. Introduction

[2] Magnetic reconnection is one of the most important mechanisms of plasma transport and energy conversion in astrophysical plasmas. In the solar atmosphere, it is related to the occurrence of flares, to coronal mass ejections, and also to coronal heating [*Priest*, 1984; *Gosling et al.*, 1995]. In the magnetosphere of the Earth, it facilitates the entry of particles and energy from the solar wind into the magnetosphere [*Sonnerup et al.*, 1981] and it is also related to the release of magnetic energy in the magnetotail [*Birn and Hesse*, 1996]. Magnetic reconnection involves the topological change of magnetic field lines in a localized region known as the diffusion zone. The appearance of a kink in the newly reconnected lines produces jets of plasma away from this region. Although in astrophysical plasmas those jets have been previously detected in situ by *Phan et al.* [2000] and *Paschmann et al.* [1979], observational evidence of the existence of the diffusion regions has been obtained only recently by *Mozer et al.* [2002].

[3] The theoretical description of magnetic reconnection processes has by and large been developed within the framework of magnetohydrodynamics (MHD). The first theoretical model for magnetic reconnection is the so called Sweet-Parker model [*Parker*, 1957]. According to Sweet-Parker, the size of the dissipation region (where the frozen-in flux constraint is broken) controls the reconnection rate (M), which scales with the Lundquist number S like $M \approx S^{-1/2}$. In many astrophysical systems, such as solar flares and magnetic substorms, S lies between 10^6 and 10^{12}, thus implying that the reconnection rate is extremely small to explain the short timescales observed in this energy transfer process. *Petschek* [1964] suggested that the reconnection rate could be increased due to the presence of MHD slow mode compressional shocks in connection with a smaller diffusion region. In Petschek's model the reconnection rate scales with S like $M \approx ln(S)^{-1}$, which implies a reconnection rate larger than Sweet-Parker's for plasmas with $S \gg 1$. However, in the last decade Petschek's model have been a subject of controversy [see, e.g., *Biskamp*, 2000; *Wang et al.*, 2000], as to whether this stationary regime is actually achieved in natural plasmas.

[4] Recent works [*Terasawa*, 1984; *Scudder*, 1997] suggest that in high-S plasmas, it is necessary to take the relative motion between different species into account, which is not distinguished in the one-fluid MHD framework. A first attempt in this direction is to include the Hall term in Ohm's law. This level of description is known as Hall-MHD. The Hall effect plays an important role in the dynamics of the magnetic field in a variety of astrophysical objects, such as dense molecular clouds, white dwarfs, or accretion disks [see, e.g., *Minnini et al.*, 2003, and references therein]. In the last few years, signatures of Hall currents have also been reported both in the Earth's magnetopause and magnetotail [*Øieroset et al.*, 2001; *Deng and Matsumoto*, 2001]. Previous studies using numerical simulations of nondriven Hall reconnection [see, e.g., *Ma and Bhattacharjee*, 2001; *Birn et al.*, 2001; *Hesse et al.*, 2001; *Otto*, 2001] find that the reconnected flux increases when the Hall term is present.

[5] In this paper we study the importance of the Hall term in externally driven magnetic reconnection. We perform numerical simulations of an incompressible 2 1/2 dimension Hall MHD code with different values of the dimensionless parameter ϵ, which measures the relative importance of the Hall current. In section 2 we write down the Hall MHD equations in 2 1/2 dimensions. The numerical details of the

0148-0227/05/2004JA010675$09.00

code are shown in section 3, and the main results are displayed in section 4. The conclusions of the present analysis are listed in section 5.

2. Hall MHD Equations in 2 1/2 Dimensions

[6] Highly conductive plasmas (i.e., $S \gg 1$) tend to develop thin and intense current sheets in their reconnection layers. Whenever the current width reaches values as low as $d_i = c/w_{pi}$ (w_{pi} is the ion plasma frequency and c is the speed of the light), it is no longer valid to neglect the Hall term in the generalized Ohm's law [*Ma and Bhattacharjee*, 2001]. For a fully ionized plasma of protons and electrons, Ohm's law can be written as

$$\boldsymbol{E} + \frac{1}{c}\boldsymbol{v} \times \boldsymbol{B} = \frac{4\pi\eta}{c^2}\,\boldsymbol{j} + \frac{1}{ne}\left(\frac{1}{c}\boldsymbol{j} \times \boldsymbol{B} - \nabla p_e\right), \tag{1}$$

where n is the electron and proton density (assuming quasi-neutrality), e is the charge of the electron, η is the electric resistivity, $\boldsymbol{B}$ is the magnetic field, $\boldsymbol{v}$ is the plasma flow velocity, and $\boldsymbol{j}$ is the electric current density. The second term of the right-hand side contains the Hall and the electron pressure (p_e) effects, which are both neglected in the MHD approximation. Assuming incompressibility (i.e., $\nabla \cdot \boldsymbol{v} = 0$), we can cast the so-called Hall-MHD equations in their dimensionless form as

$$\partial_t \boldsymbol{v} + (\boldsymbol{v} \cdot \nabla)\boldsymbol{v} = (\nabla \times \boldsymbol{B}) \times \boldsymbol{B} - \nabla p + \frac{1}{R}\nabla^2 \boldsymbol{v}, \tag{2}$$

$$\partial_t \boldsymbol{B} = \nabla \times [(\boldsymbol{v} - \epsilon \nabla \times \boldsymbol{B}) \times \boldsymbol{B}] + \frac{1}{S}\nabla^2 \boldsymbol{B}, \tag{3}$$

$$\nabla \cdot \boldsymbol{B} = 0 = \nabla \cdot \boldsymbol{v}. \tag{4}$$

[7] In equations (2)–(3) we have normalized $\boldsymbol{B}$ to a typical magnetic intensity B_0, $\boldsymbol{v}$ to the Alfvén speed $v_a = B_0/\sqrt{4\pi m_i n}$, the total gas pressure p to ρv_a^2, longitudes to $L_0/2\pi$ (where L_0 is the typical length of the system), and times to L_0/v_a. The Reynolds number is $R = L_0 v_a/\nu$ and $S = L_0 v_a/\eta$ is the Lundquist number. The dimensionless coefficient ϵ is defined as

$$\epsilon = \frac{c}{\omega_{pi} L_0}, \tag{5}$$

and measures the relative strength of the Hall effect. The dimensionless electron velocity is

$$\boldsymbol{v_e} = \boldsymbol{v} - \epsilon \nabla \times \boldsymbol{B}. \tag{6}$$

From equation (3) it is apparent that in the nondissipative limit (i.e., $S \to \infty$) the magnetic field remains frozen to the electron flow $\boldsymbol{v_e}$ rather than to the bulk velocity $\boldsymbol{v}$.

3. Numerical Simulations

[8] The incompressible Hall MHD simulations reported in this paper are carried out under the geometric approximation known as 2 1/2-D (two and a half dimensions). This approximation is based on the assumption that there is translational symmetry along the $\hat{\boldsymbol{z}}$ coordinate (i.e., $\partial_z = 0$). Therefore the solenoidal magnetic and velocity fields can be represented as

$$\boldsymbol{B} = \nabla \times [\hat{\boldsymbol{z}} a(x, y, t)] + \hat{\boldsymbol{z}} b(x, y, t), \tag{7}$$

$$\boldsymbol{v} = \nabla \times [\hat{\boldsymbol{z}} \phi(x, y, t)] + \hat{\boldsymbol{z}} u(x, y, t), \tag{8}$$

where $a(x, y, t)$ is the magnetic flux function and $\phi(x, y, t)$ is the stream function. In this approximation, the Hall MHD equations take the form

$$\partial_t a = [\phi - \epsilon b, a] + \frac{1}{S}\nabla^2 a + E(x, y), \tag{9}$$

$$\partial_t b = [\phi, b] + [u - \epsilon j, a] + \frac{1}{S}\nabla^2 b, \tag{10}$$

$$\partial_t w = [\phi, w] + [j, a] + \frac{1}{R}\nabla^2 w, \tag{11}$$

$$\partial_t u = [b, a] + [\phi, u] + \frac{1}{R}\nabla^2 u. \tag{12}$$

The nonlinear terms are the standard Poisson brackets (i.e., $[p, q] = \partial_x p\, \partial_y q - \partial_y p\, \partial_x q$), $j = -\nabla^2 a$ is the $\hat{\boldsymbol{z}}$-component of the electric current density, and $w = -\nabla^2 \phi$ is the $\hat{\boldsymbol{z}}$-component of the flow vorticity. Both the total and electron pressures are absent from the formulation, but they have not been neglected. They can both be computed a posteriori from their respective Poisson equations (in terms of the velocity and magnetic fields), as it is standard practice in incompressible hydrodynamics [*McComb*, 1990].

[9] We performed numerical integrations of equations (9)–(12). The computation is carried out in a rectangular domain assuming periodic boundary conditions. The spatial coordinates span the ranges $-\pi \le x, y \le \pi$. The magnetic vector potential $a(x, y, t)$, the stream function $\phi(x, y, t)$, and $\hat{\boldsymbol{z}}$-components of the magnetic field $b(x, y, t)$ and velocity field $u(x, y, t)$ are expanded in their corresponding spatial Fourier amplitudes $a_{\boldsymbol{k}}(t)$, $\phi_{\boldsymbol{k}}(t)$, $b_{\boldsymbol{k}}(t)$, and $u_{\boldsymbol{k}}(t)$. The equations for these Fourier amplitudes are evolved in time using a second-order Runge-Kutta scheme and the nonlinear terms are evaluated following a 2/3 dealiased pseudospectral technique.

[10] We apply a steady external forcing, $E(x, y)$, on equation (9), keeping zero magnetic and velocity fields as initial conditions for all our simulations. In next section we give the details of the external forcing. The Reynolds numbers for the runs reported here are $R = S = 100$ and the spatial size of the simulations is 384×384 grid points.

4. Driven Hall Magnetic Reconnection

[11] Numerical simulations of nondriven Hall reconnection have been performed by previous authors [e.g., *Ma and Bhattacharjee*, 2001; *Birn et al.*, 2001; *Hesse et al.*, 2001; *Otto*, 2001]. These simulations systematically show the growth of the reconnection rate as the Hall parameter is increased. In the present paper we want to simulate externally driven reconnection, to imitate for instance the

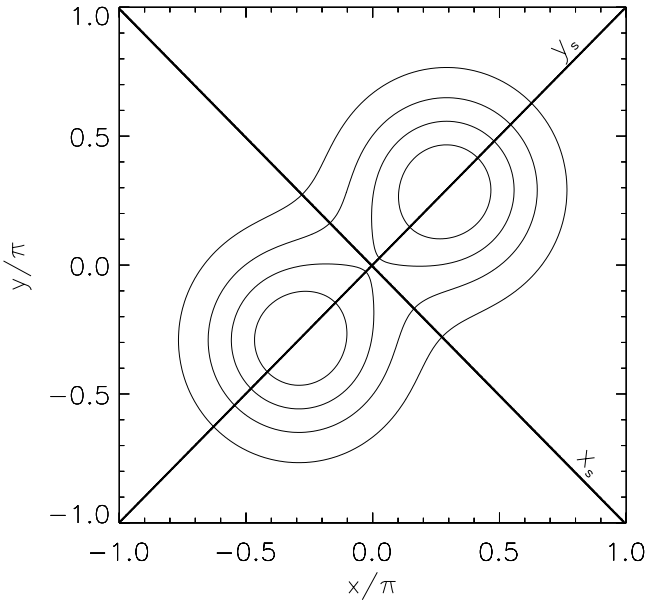

Figure 1. Contour levels of the forcing term given in equation (13) at [0.2, 0.4, 0.6, 0.8] E_0. The coordinates along (x_s) and across (y_s) the current sheet are also displayed as a reference.

conditions of magnetic flux of solar origin hitting the magnetopause.

[12] In order to provide a physical scenario of driven reconnection, the present simulations assume the following external forcing on equation (9):

$$E(x,y) = E_0\left\{\exp\left[-\frac{(x-x_1)^2+(y-y_1)^2}{d^2}\right] + \exp\left[-\frac{(x-x_2)^2+(y-y_2)^2}{d^2}\right]\right\} \quad (13)$$

which physically represents two kernels of an external stationary electric field $E(x, y)\,\hat{z}$ of equal intensity, centered at $(x_1, y_1) = (0.3\pi, 0.3\pi)$ and $(x_2, y_2) = (-0.3\pi, -0.3\pi)$, and with a kernel width $d = 0.375\pi$, as sketched in Figure 1.

[13] The dawn-dusk electric field intensity is $E = u_{SW}B_0/c$, where u_{SW} is the solar wind velocity. For a typical magnetic field of 10–50 nT, electron densities of 10 cm^{-3}, and solar wind velocities of 10^7 cm s^{-1}, we estimate the dimensionless intensity of the external forcing $E_0 = u_{SW}/v_a$ (see equation (13)) to be anywhere between $E_0 = 0.2$ and $E_0 = 1$. We therefore set the forcing intensity at a moderate value of $E_0 = 0.3$ throughout this paper.

[14] In this section we present our numerical results and study several aspects of externally driven reconnection events. We present results obtained for different values of the Hall coefficient ($\epsilon = 0, 0.1, 0.5, 1$). The results presented here include the global structure of the magnetic field, current, and flow field as well as the time evolution of the reconnection rate.

4.1. Current Layer

[15] In Figure 2 we present contour plots of the magnetic flux $a(x, y)$, the stream function $\phi(x, y)$, and the $\hat{z}$-components of the magnetic and velocity fields (i.e., $b(x, y)$ and $u(x, y)$) for the case $\epsilon = 0.1$ at time $t = 3.6$.

[16] The magnetic flux and stream function show the typical behavior expected for a two-dimensional magnetic reconnection scenario. The magnetic field component along $\hat{z}$ exhibits a characteristic quadrupole pattern, which has been reported in the literature as a clear signature of Hall MHD reconnection [*Sonnerup et al.*, 1981; *Terasawa*, 1984].

[17] Current sheets are shown in Figure 3, where we display the electric current density j obtained for different values of ϵ. Each plot is made at the time when the current density reaches its maximum value; for $\epsilon = 0$, 0.1, 0.5, and 1, the maximum j (at the center of the current sheet) resulted 45, 50, 28, and 19, respectively.

[18] We note that as ϵ increases, the formation of the current sheet is accelerated and the size of the current sheet decreases, as can readily be seen by comparing the width and length of the current density distribution for $\epsilon = 0$ and $\epsilon = 0.1$ (see Figure 3). Also, note that for the case $\epsilon = 0$ the current layer is long, while for $\epsilon \neq 0$ the current sheet progressively shrinks.

4.2. Electronic Diffusion Region

[19] As mentioned in section 2, for an ideal plasma the magnetic field is frozen to the electron flow rather than to the bulk flow. The two upper panels in Figure 4 show electron and ion velocity profiles across the current sheet, i.e., along y_s (see Figure 1). The lower panels in Figure 4 show velocity profiles along the sheet, i.e., along x_s. The left panels correspond to the case $\epsilon = 0.1$ at $t = 3.6$, while the right panels correspond to $\epsilon = 1.0$ and $t = 2.0$, which are the times when the current density reaches its maximum at its center. Figure 4 suggests that there is a zone where electron velocities are several times larger than the ion velocities. This Hall zone is characterized by the demagnetization of ions, while the magnetic field remains frozen to the electron flow.

[20] To identify the Hall-dominated region in the (x, y) plane, we plot (see Figure 5) the contours of the ratio

$$\left|\frac{v_e}{v}\right| = \left|\frac{v-\epsilon j}{v}\right|. \quad (14)$$

The case shown in Figure 5 corresponds to the run where $\epsilon = 0.5$ (at time $t = 2.0$) and shows a small region localized at the center of the current sheet, where the electron flow is approximately 10 times faster than the ion flow (dark shadow). Surrounding this small zone, we can identify a larger region where the electron flow is larger than twice the ion flow (light shadow). The intermediate region corresponds to electrons five time faster than ions. Also in Figure 5 we have plotted contours of the out-of-plane magnetic field component b for reference. We note that the quadrupolar symmetry of b (x, y, t) agrees with the zone where the electron flow approximately duplicates the ion flow. This region is therefore the zone where the decoupling between electrons and ions is maximum and where the Hall current is definitely nonnegligible.

4.3. Reconnection Rate

[21] The reconnected magnetic flux (F) per unit length (along z) can be computed from the difference of the values

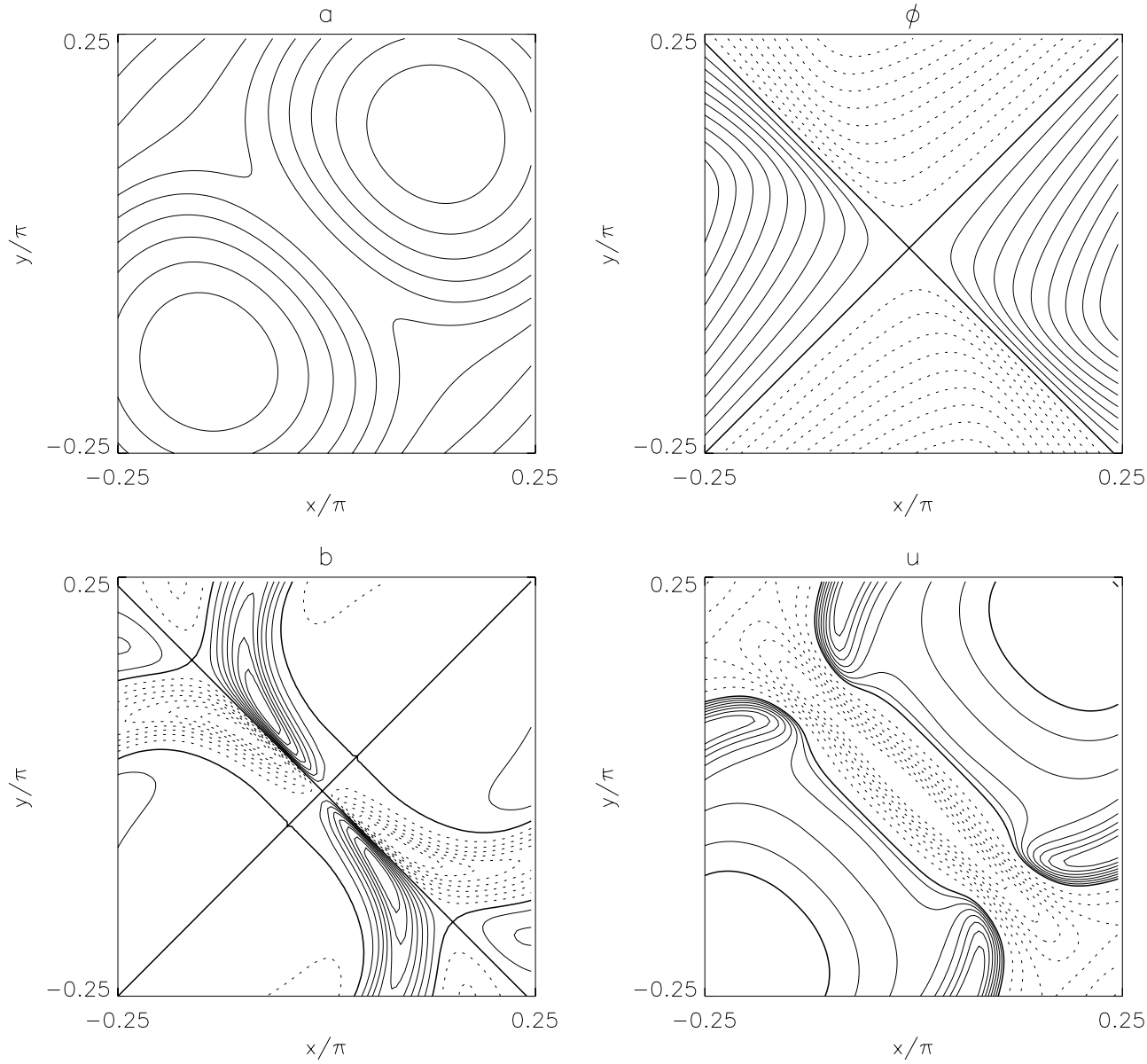

Figure 2. Contours of magnetic flux ($a(x, y)$), stream function ($\phi(x, y)$), and magnetic ($b(x, y)$) and velocity field ($u(x, y)$) components along $\hat{\mathbf{z}}$ in a zoom of the central portion of the (x, y) plane at $t = 3.6$ for the case $\epsilon = 0.1$. Solid (dotted) lines correspond to positive (negative) levels.

of the magnetic flux function (a) at the X point (reconnection site) and at the O point (center of the kernel). Thus the rate of F can be obtained from

$$\frac{dF}{dt} = \frac{d}{dt}\Delta a \equiv \frac{d}{dt}(a_X - a_O). \tag{15}$$

From equation (9), and noting that X and O are magnetic null points (i.e., $\partial_x a = \partial_y a = 0$), we obtain

$$\frac{dF}{dt} = \Delta E - \frac{1}{S}\Delta j \equiv (E_X - E_O) - \frac{1}{S}(j_X - j_O), \tag{16}$$

which expresses the fact that the external forcing injects an amount of magnetic flux per unit time equal to ΔE, while the reconnection process destroys an amount of magnetic flux per unit time equal to $\Delta j/S$. We therefore define the reconnection rate at the X-point simply as

$$M = \frac{1}{S} j_X. \tag{17}$$

In Figure 6 we plot the reconnection rate as a function of time for the various values of ϵ considered. It seems apparent that as the relative importance of the Hall effect is increased, (1) the growth of the reconnection rate is initially faster, (2) the time for saturation is shorter, and (3) the saturation level is lower.

5. Conclusions

[22] In this paper we present results from externally driven magnetic reconnection simulations, within the frame-

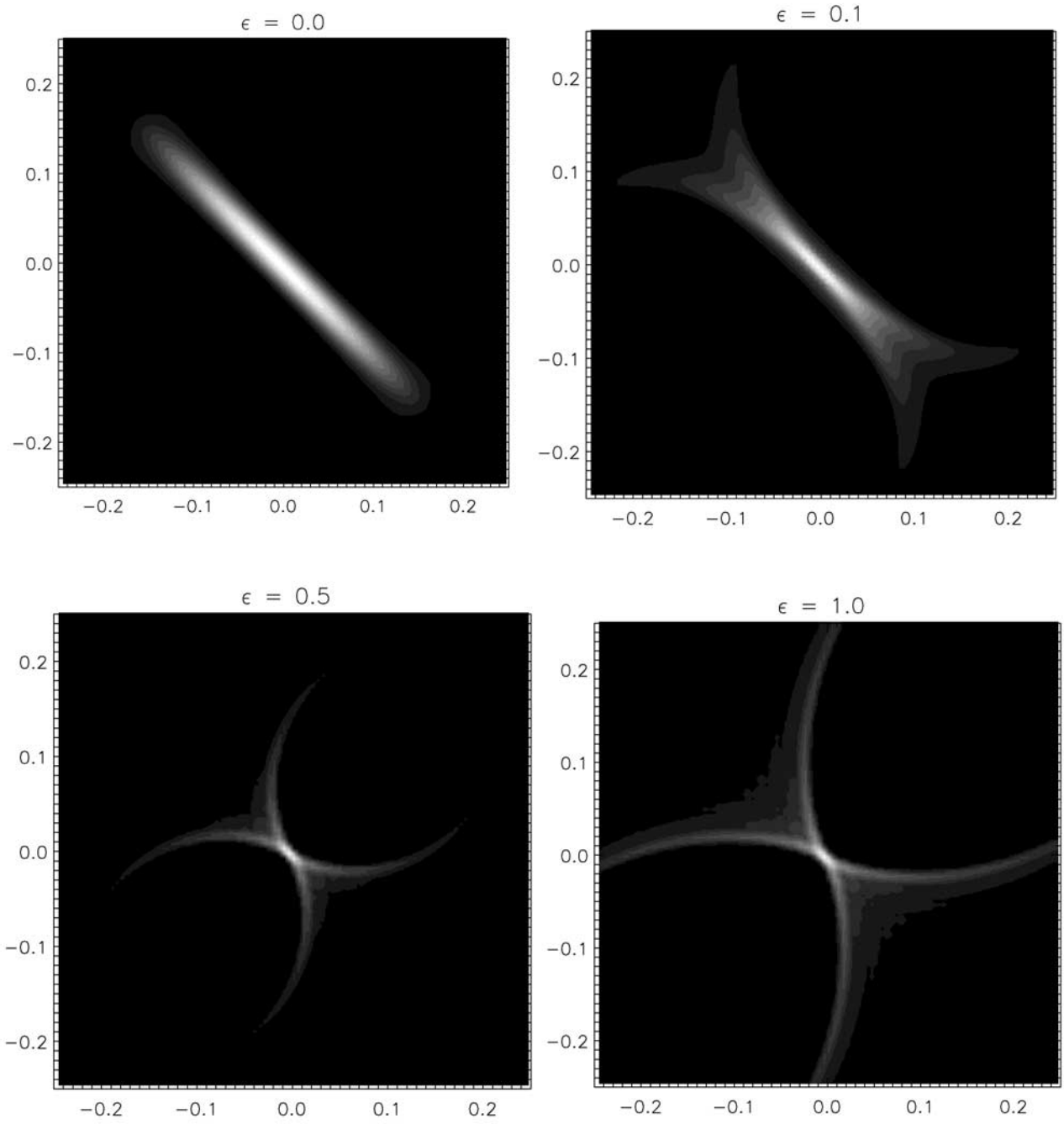

Figure 3. Current density in a zoom of the central portion of the (x, y) plane for $\epsilon = 0.0, 0.1, 0.5, 1.0$ as indicated. Each frame corresponds to the time where the current density at the center is maximum, i.e., $t = 3.8$, $t = 3.6$, $t = 3.2$, and $t = 2.0$, respectively (see also Figure 6). The color map in each panel is normalized to the maximum value of their own current distribution.

work of incompressible Hall MHD in $2\frac{1}{2}$ dimensions. We quantitatively assess the importance of the Hall current in the reconnection process by performing a set of simulations with different values of the Hall parameter.

[23] Simulations of nondriven Hall reconnection [e.g., *Ma and Bhattacharjee*, 2001; *Birn et al.*, 2001; *Hesse et al.*, 2001; *Otto*, 2001] have shown the increase of the reconnection rate as the Hall parameter is increased. In the present analysis, we decided instead to maintain an external source of magnetic flux at two kernels (see equations (9) and (13)) to imitate the conditions of magnetic reconnection at the Earth's magnetopause. For typical values of the magnetopause environment, we find that the ensuing reconnection process does not reach a stationary regime. We find that as the relative importance of the Hall effect is increased, the growth of the reconnection rate is initially faster, in

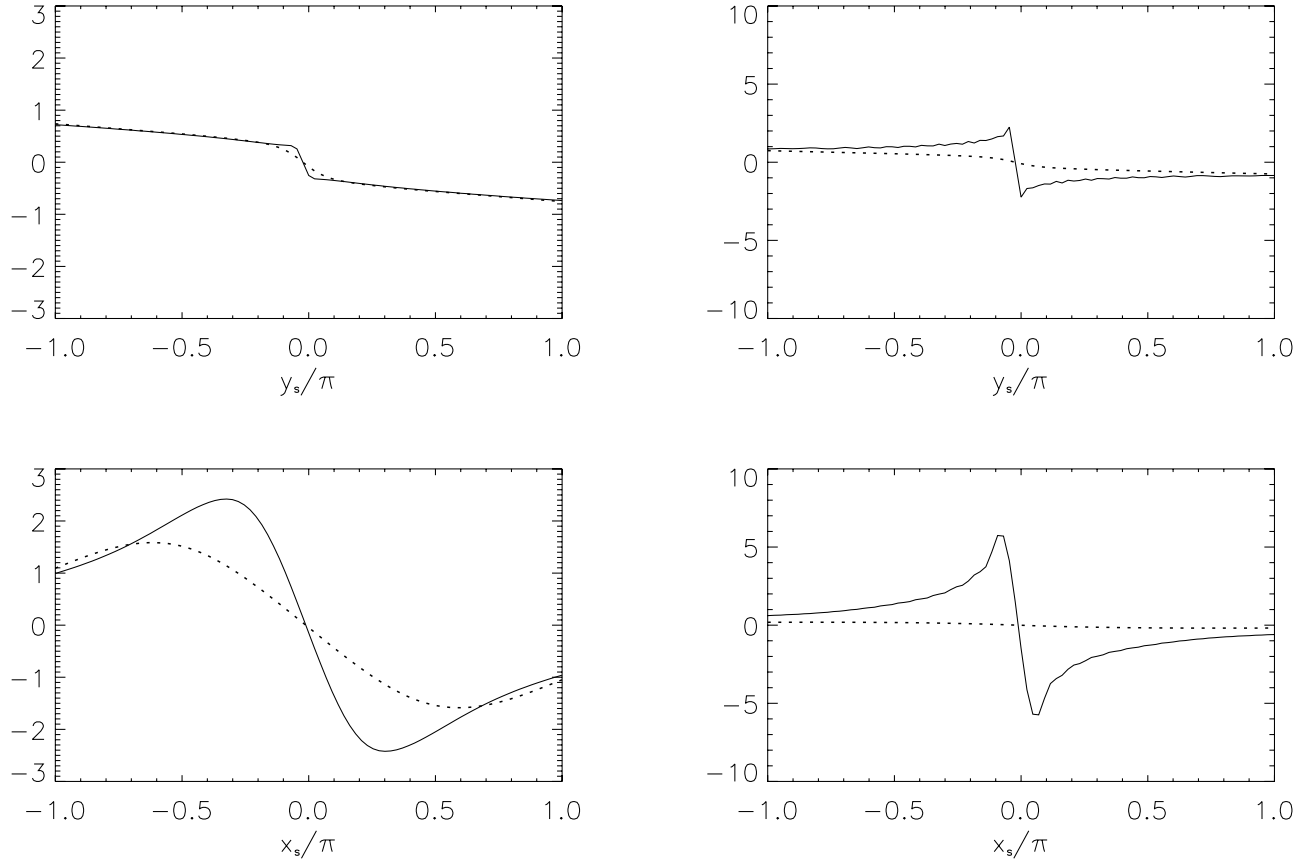

Figure 4. Electron (solid line) and ion (dashed line) velocity profiles. (top) Profiles across the current sheet (i.e., along y_s, see Figure 1) and (bottom) profiles along the sheet (i.e., along x_s), where (left) $\epsilon = 0.1$ at $t = 3.6$ and (right) $\epsilon = 1.0$ at $t = 2.0$.

qualitative agreement with the nondriven cases. However, we also observe that as the Hall parameter is increased, the reconnection process reaches saturation on shorter timescales and at correspondingly lower levels. Therefore the total reconnected flux in a given reconnection event becomes smaller as the Hall parameter is increased.

[24] A tentative explanation for this behavior is the following. In Hall MHD, the magnetic field lines are dragged to the diffusion region by the electron flow. Since electrons enter the diffusion region at a much faster speed, it seems reasonable that the reconnection rate becomes larger. However, this higher speed can also cause the field lines to pile up at the entrance of the diffusion region, thus quenching the reconnection process at a lower level.

[25] The flux pileup of antiparallel magnetic field merging is addressed in a recent paper by *Dorelli* [2003]. Assuming a stationary and irrotational flow in Hall-MHD, *Dorelli* [2003] obtains analytical solutions for the magnetic field around a stagnation point. In this approximation, increasing the value of the Hall parameter ϵ leads to a reduction of the magnetic energy piled up just upstream of the reconnection region. Therefore according to the Bernoulli condition (which stems from the Navier-Stokes equation for stationary and irrotational flows), a smaller pressure drop is required to maintain a given reconnection rate. However, when nonstationary regimes are considered,

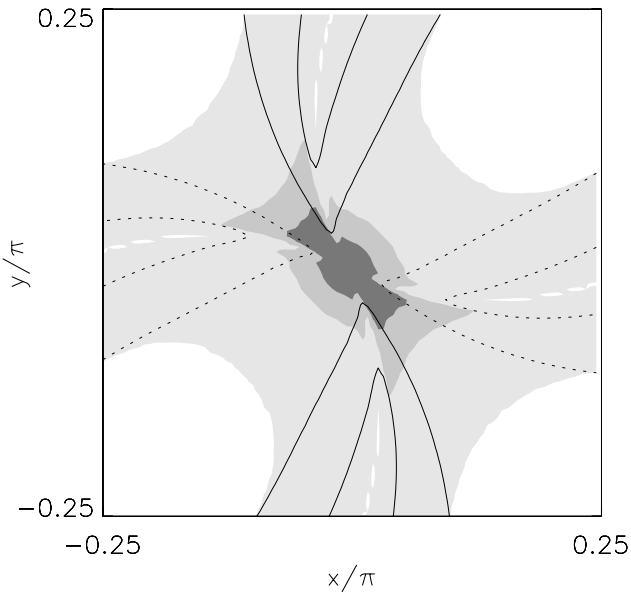

Figure 5. Three contour levels in different shades for the ratio of electron velocity to ion velocity: $|v_e/v| = 2$ (light), 5 (intermediate), and 10 (dark), for the case $\epsilon = 0.5$ at $t = 2.0$. The quadrupolar structure of b is overlaid for reference.

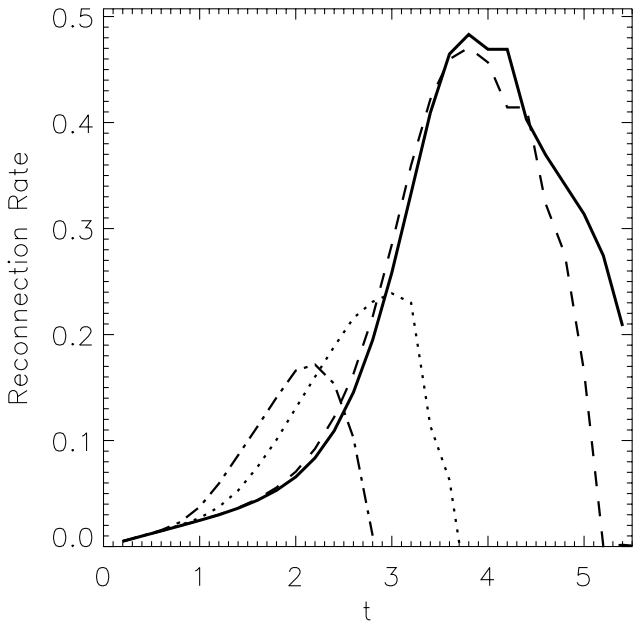

Figure 6. Reconnection rate as a function of time for different values of ϵ. The solid curve corresponds to $\epsilon = 0$, followed by $\epsilon = 0.1$ (– – –), $\epsilon = 0.5$ (. . .), and $\epsilon = 1.0$ (–.–.–.).

the reconnection rate is quashed at a lower level as the Hall parameter is increased.

[26] An alternative explanation for the reduction of the reconnection rate caused by the addition of Hall currents was given by *Craig et al.* [2003]. They find that the nature of the reconnection process changes appreciably whenever $\epsilon^2 S \gg 1$, which is confirmed by our simulations. Our run $\epsilon = 0.1$ is a marginal case (since $\epsilon^2 S \approx 1$) where only slight changes are observed when compared with pure MHD, while the remaining runs show important departures from MHD. Assuming a quasi-one dimensional current sheet, *Craig et al.* [2003] find a reduction of the reconnection rate as the Hall parameter is increased, as well as an increase of the energy dissipation rate caused by the formation of multiple current layers in the surroundings of the main reconnection site.

[27] In summary, because of the nonlinear nature of the reconnection process, the presence of the Hall current does not necessarily enhance the total reconnected flux. These various recent studies on the role of Hall currents on magnetic reconnection clearly show that this is a very active area of research and that further work is certainly required to obtain a better understanding.

[28] **Acknowledgments.** The authors would like to thank to the referees for their comments. This work was supported by the University of Buenos Aires through grants UBACyT X209 and by the Agencia Nacional de Promoción de Ciencia y Tecnología through grant PIP2000 03/9483. S. D. and D. O. G. are members of the Carrera del Investigador Científico, CONICET.

[29] Shadia Rifai Habbal thanks both referees for their assistance in evaluating this paper.

References

Birn, J., and M. Hesse (1996), Details of current disruption and diversion in simulations of magnetotail dynamics, *J. Geophys. Res.*, *101*, 15,345.

Birn, J., et al. (2001), Geospace Environmental Modeling (GEM) magnetic reconnection challenge, *J. Geophys. Res.*, *106*, 3715.

Biskamp, D. (2000), *Magnetic Reconnection in Plasmas*, *Cambridge Monogr. on Plasma Phys.*, Cambridge Univ. Press, New York.

Craig, I. J. D., J. Heerikhuisen, and P. G. Watson (2003), Hall current effects in dynamic magnetotail reconnection solutions, *Phys. Plasmas*, *10*, 3120.

Deng, X. H., and H. Matsumoto (2001), Rapid magnetic reconnection in the Earth's magnetosphere mediated by whistler waves, *Nature*, *410*, 557.

Dorelli, J. C. (2003), Effects of Hall electric fields on the saturation of forced antiparallel magnetic field margin, *Phys. Plasmas*, *10*, 3309.

Gosling, J. T., J. Birn, and M. Hesse (1995), Three-dimensional magnetic reconnection and the magnetic topology of coronal mass ejection events, *Geophys. Res. Lett.*, *22*, 869.

Hesse, M., J. Birn, and M. Kuznetsova (2001), Collisionless magnetic reconnection: Electron processes and transport modeling, *J. Geophys. Res.*, *106*, 3721.

Ma, Z., and A. Bhattacharjee (2001), Hall magnetohydrodynamic reconnection: The Geospace Environment Modeling challenge, *J. Geophys. Res.*, *106*, 3773.

McComb, W. D. (1990), *The Physics of Fluid Turbulence*, Clarendon Press, Oxford, UK.

Minnini, P., D. O. Gomez, and S. M. Mahajan (2003), Dynamo action in magnetohydrodynamics and Hall-magnetohydrodynamics, *Astrophys. J.*, *584*, 1120.

Mozer, F., S. Bale, and T. D. Phan (2002), Evidence of diffusion regions at a subsolar magnetopause crossing, *Phys. Rev. Lett.*, *89* 015002.

Øieroset, M., et al. (2001), In situ detection of collisionless reconnection in the Earth's magnetotail, *Nature*, *412*, 414.

Otto, A. (2001), Geospace Environment Modeling (GEM) magnetic reconnection challenge: MHD and Hall-MHD constant and current dependent resistivity models, *J. Geophys. Res.*, *106*, 3751.

Parker, E. N. (1957), Sweet's mechanism for merging magnetic fields in conducting fluids, *J. Geophys. Res.*, *62*, 509.

Paschmann, G., et al. (1979), Plasma acceleration at the Earth's magnetopause: Evidence for reconnection, *Nature*, *282*, 243.

Petschek, H. E. (1964), Magnetic annihilation, in *AAS/NASA Symposium on the Physics of Solar Flares*, edited by W. N. Ness, p. 425, NASA, Washington, D. C.

Phan, T. D., et al. (2000), Evidence for an extended reconnection line at the dayside magnetopause, *Nature*, *404*, 848.

Priest, E. R. (1984), Magnetic reconnection at the Sun, in *Magnetic Reconnection in Space and Laboratory Plasmas*, *Geophys. Monogr. Ser.*, vol. 30, edited by E. W. Hones, p. 63, AGU, Washington, D. C.

Scudder, J. (1997), Theoretical approaches to the description of magnetic merging: The need for finite, anisotropic, ambipolar Hall MHD, *Space Sci. Rev.*, *80*, 235.

Sonnerup, B. U. O., et al. (1981), Evidence for magnetic field reconnection at the Earth's magnetopause, *J. Geophys. Res.*, *86*, 10,049.

Terasawa, T. (1984), Hall current effect on tearing mode instability, *Geophys. Res. Lett.*, *10*, 475.

Wang, X., A. Bhattacharje, and Z. W. Ma (2000), Collisionless reconnection: Effects of Hall current and electron pressure gradient, *J. Geophys. Res.*, *105*, 27,633.

S. Dasso, D. O. Gómez, and L. F. Morales, Instituto de Astronomía y Física del Espacio (IAFE) CC 67 Suc. 28, 1428 Buenos Aires, Argentina. (dasso@df.uba.ar)